

Regulation of actin dynamics by annexin 2

Matthew J Hayes¹, Dongmin Shao¹,
Maryse Bailly and Stephen E Moss*

Division of Cell Biology, Institute of Ophthalmology, University College London, London, UK

Annexin 2 is a ubiquitous Ca²⁺-binding protein that is essential for actin-dependent vesicle transport. Here, we show that in spontaneously motile cells annexin 2 is concentrated in dynamic actin-rich protrusions, and that depletion of annexin 2 using siRNA leads to the accumulation of stress fibres and loss of protrusive and retractile activity. Cells co-expressing annexin 2-CFP and actin-YFP exhibit Ca²⁺-dependent fluorescence resonance energy transfer throughout the cytoplasm and in membrane ruffles and protrusions, suggesting that annexin 2 may directly interact with actin. This notion was supported by biochemical studies, in which we show that annexin 2 reduces the polymerisation rate of actin monomers in a dose-dependent manner. By measuring actin polymerisation rates in the presence of barbed-end and pointed-end cappers, we further demonstrate that annexin 2 specifically inhibits filament elongation at the barbed ends. These results show that annexin 2 has an essential role in maintaining the plasticity of the dynamic membrane-associated actin cytoskeleton, and that its activity in this context may be at least partly explained through direct interactions with polymerised and monomeric actin.

The EMBO Journal (2006) 25, 1816–1826. doi:10.1038/sj.emboj.7601078; Published online 6 April 2006

Subject Categories: membranes & transport; cell & tissue architecture

Keywords: actin; annexin; calcium; capping protein; cytoskeleton

Introduction

Annexin 2 is one of a family of conserved Ca²⁺-binding proteins, members of which are expressed in virtually all eukaryotic cell types (Gerke *et al*, 2005). The unifying biochemical property of annexins, namely their ability to bind to negatively charged phospholipids in the presence of Ca²⁺, suggests that annexin function is likely to involve membrane dynamics. For annexin 2 there is evidence to support such a role, both in the secretory pathway (Drust and Creutz, 1988; Ali *et al*, 1989) and endocytic pathway, where it has been shown to associate with early endosomes (Emans *et al*, 1993; Harder *et al*, 1997; Jost *et al*, 1997). It has also been found

on phagosomes (Diakonova *et al*, 1997) and actin-propelled pinosomes (Merrifield *et al*, 2001) via an interaction with phosphatidylinositol 4,5-bisphosphate (Hayes *et al*, 2004a, b). Disruption of annexin 2 function, either by expression of a dominant-negative mutant or by RNA interference, leads to perturbations in endocytic and secretory pathways (Harder and Gerke, 1993; Knop *et al*, 2004).

In most cells, annexin 2 is present both as a cytosolic monomer and as a heterotetrameric complex comprising two molecules of annexin 2 and two of S100A10 (Johnsson *et al*, 1988). The heterotetramer locates constitutively to the membrane-cytoskeleton where, given recent observations identifying interactions between S100A10 and various cell surface receptors and ion channels (Nilius *et al*, 1996; Okuse *et al*, 2002; van der Graaf *et al*, 2003), it may be involved in the organisation of receptor cytoplasmic domains with the subplasma membrane cytoskeleton. On the other hand, monomeric annexin 2 does not require S100A10 to bind to endosomes (Konig and Gerke, 2000), and is more likely to be involved in dynamic interactions with lipid microdomains (Babiychuk and Draeger, 2000). Annexin 2 has also been shown to be associated with and necessary for the formation of actin-rich tight junctions (Lee *et al*, 2004), and has been proposed to regulate cell–cell contacts through formation of complexes with Rac1/p21-associated kinase and cadherin (Hansen *et al*, 2002).

The close association of annexin 2 with both the actin cytoskeleton and dynamic cellular membranes led us to test the possibility that annexin 2 may have a more direct influence on actin polymerisation than has previously been assumed. Here, we demonstrate that annexin 2 is concentrated in dynamic actin-rich protrusions, and that in cells depleted of annexin 2 ruffling and protrusive activity are virtually abolished. We further show that annexin 2 binds to G-actin and interferes with the barbed-end growth of actin filaments. Annexin 2 may thus provide a direct structural link between the growing ends of actin filaments and the plasma membrane.

Results

Annexin 2 is localised to regions of cells undergoing actin remodelling

To examine the association of annexin 2 with actin-rich structures, we transfected MIO Müller cells with annexin 2-GFP and then imaged the living cells using confocal microscopy. MIO is a nontransformed cell line (Limb *et al*, 2002) that exhibits intrinsic membrane ruffling. We observed marked enrichment of annexin 2-GFP at membrane ruffles, but not in adjacent stationary areas at the cell periphery. The boxed area of the cell in Figure 1A illustrates this point, the time-lapse sequence showing that the loss of annexin 2-GFP is associated with the disappearance of the ruffle. Co-expression of CFP alone (a cell volume control) with annexin 2-YFP revealed enrichment of the latter but not the former in ruffles (Figure 1B). This is confirmed quantitatively by analysis of

*Corresponding author. Division of Cell Biology, Institute of Ophthalmology, University College London, 11-43 Bath Street, London EC1V 9EL, UK. Tel.: +44 207 608 6973; Fax: +44 207 608 4034; E-mail: s.moss@ucl.ac.uk

¹These authors contributed equally to this work

Received: 26 October 2005; accepted: 13 March 2006; published online: 6 April 2006

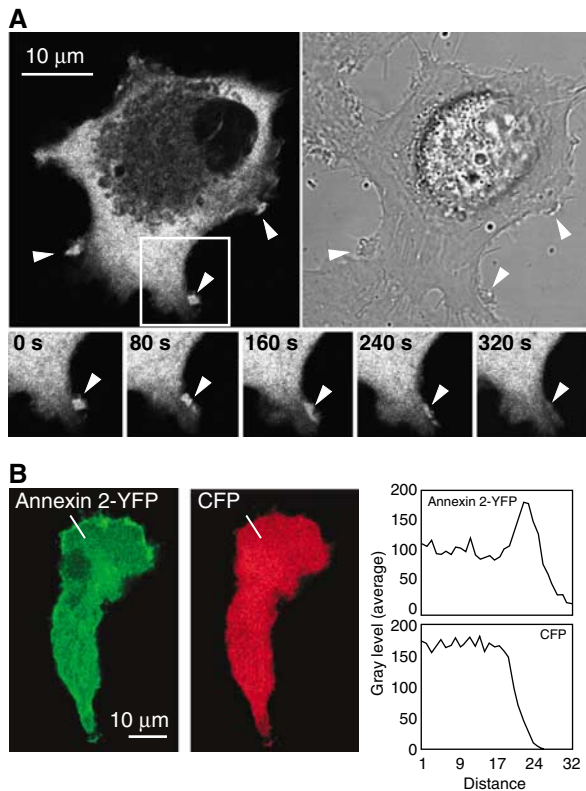


Figure 1 Annexin 2 is concentrated in membrane ruffles in MIO cells. **(A)** Müller cells were transiently transfected with annexin 2-GFP prior to time-lapse confocal and phase image acquisition. Arrowheads point to the enrichment of annexin 2-GFP in dynamic membrane ruffles. The timed series elaborating the boxed area in **(A)** shows that loss of annexin 2-GFP is coincident with the collapse of these structures and cessation of ruffling. **(B)** Müller cells were transiently co-transfected with pECFP-C1 and annexin 2-YFP. The following day the cells were fixed with 3.7% paraformaldehyde and prepared for confocal microscopy. Thin section scans were obtained (approximately 0.2 µm in thickness near the base of the cells) using a Leica AOB system. Images were quantified using the 'linescan' function of Metamorph. Annexin 2 but not CFP is enriched in the extending ruffles.

line scans through such ruffles, and shows that the increased fluorescence intensity of annexin 2 at these regions is not due to increased membrane thickness. In experiments using MTLn3 cells fixed at a series of time points following plating, we also observed co-localisation of annexin 2 and F-actin at the ruffles of spreading cells, which diminished once spreading had finished and the F-actin reorganised into stress fibres (Supplementary Figure 1). These observations suggest that annexin 2 predominantly co-localises with actin at regions of active cytoskeletal remodelling.

To determine if annexin 2 has a functional role in membrane ruffling, we examined the effects on the actin cytoskeleton of siRNA-mediated depletion of annexin 2. Western blots of extracts prepared from cells cultured for 4 days in the presence or absence of 60 pmol/ml siRNA for annexin 2 revealed marked depletion of annexin 2 but no change in the levels of annexin 1, α -tubulin or actin (Figure 2A). Immunofluorescence microscopy showed that the treated cell population contained some cells that were unaffected, and a majority in which annexin 2 was virtually undetectable (Figure 2B). The most striking phenotype of the cells depleted

of annexin 2 was a massive accumulation of stress fibres concomitant with the loss of cortical actin and the disappearance of actin-rich ruffles. This reorganisation of actin appeared in a manner temporally coincident with the loss of annexin 2, when examined in cells maintained in siRNA over a period of 6 days (Supplementary Figure 2). Annexin 2-depleted cells also became remarkably flattened (Figures 2B and C), although no difference was observed in total cellular volume when the cells were examined by FACS (data not shown). Quantitative analysis (described in detail in Figure 3) allowed us to establish that annexin 2-depleted cells have a mean footprint approximately one order of magnitude greater than control cells. This striking difference in size enabled us to differentiate control and annexin 2-depleted cells within a mixed population of living cells, with close to 100% confidence. Knockdown of annexin 2 in ARPE19 retinal epithelial cells and Rat1 fibroblasts also resulted in a stress-fibre-dominated, flattened cellular phenotype (data not shown). Co-staining with paxillin showed that the abundant actin stress fibres in the annexin 2-depleted cells are tethered to focal adhesions, suggesting that they are physiologically normal (Figure 2C). Thus, the absence of annexin 2 is associated with the loss of dynamic actin-based structures, and the proliferation, thickening and reinforcement of more stable actin filament structures.

In order to test if the anomalous F-actin phenotype was a direct consequence of annexin 2 depletion rather than a more remote downstream effect, we performed experiments aimed at phenotypic reversal using a 'hardened' annexin 2-GFP expression construct (hd-anx2-GFP), in which three silent point mutations were introduced into the annexin 2 cDNA at the siRNA target site. Cells were cultured in the presence of annexin 2 siRNA for 2 days and then transfected either with hd-anx2-GFP or GFP before fixation and immunofluorescence microscopy (Figure 2D). Quantitative analysis revealed that >95% of cells that immunostained positively with antisera to annexin 2 exhibited a normal phenotype ($n=83$, Figures 2D (pink arrowhead) and 2E), whereas >90% of cells negative for annexin 2 displayed the knockdown phenotype ($n=219$, Figures 2D (yellow arrowheads) and 2E). In cells expressing hd-anx2-GFP, all of which also stained positively with antisera to annexin 2, >90% exhibited a normal phenotype ($n=35$, Figure 2E). In cultures transfected with GFP alone, approximately 85% of cells that were GFP positive but annexin 2 negative displayed the knockdown phenotype ($n=22$, Figure 2E). Time-lapse imaging of such cells expressing hd-anx2-GFP confirmed that reversal of the morphological phenotype was accompanied by restoration of membrane ruffling and protrusive activity (Supplementary Figure 3). These results confirm that the siRNA-resistant annexin 2-GFP, but not GFP, is able to reverse the F-actin phenotype observed in annexin 2-depleted cells.

Since part of the cellular pool of annexin 2 associates *in vivo* with S100A10, we also examined the consequences of annexin 2 depletion on S100A10 expression, and of S100A10 depletion on annexin 2 expression and the F-actin phenotype. Whereas cells depleted of annexin 2 showed a reduction in the level of expression of S100A10 (Figure 2F), which is consistent with previous studies demonstrating co-regulation of expression of annexin 2 and S100A10 (Puisieux *et al*, 1996), depletion of S100A10 using siRNA altered neither annexin 2 expression nor the F-actin phenotype (Figure 2G).

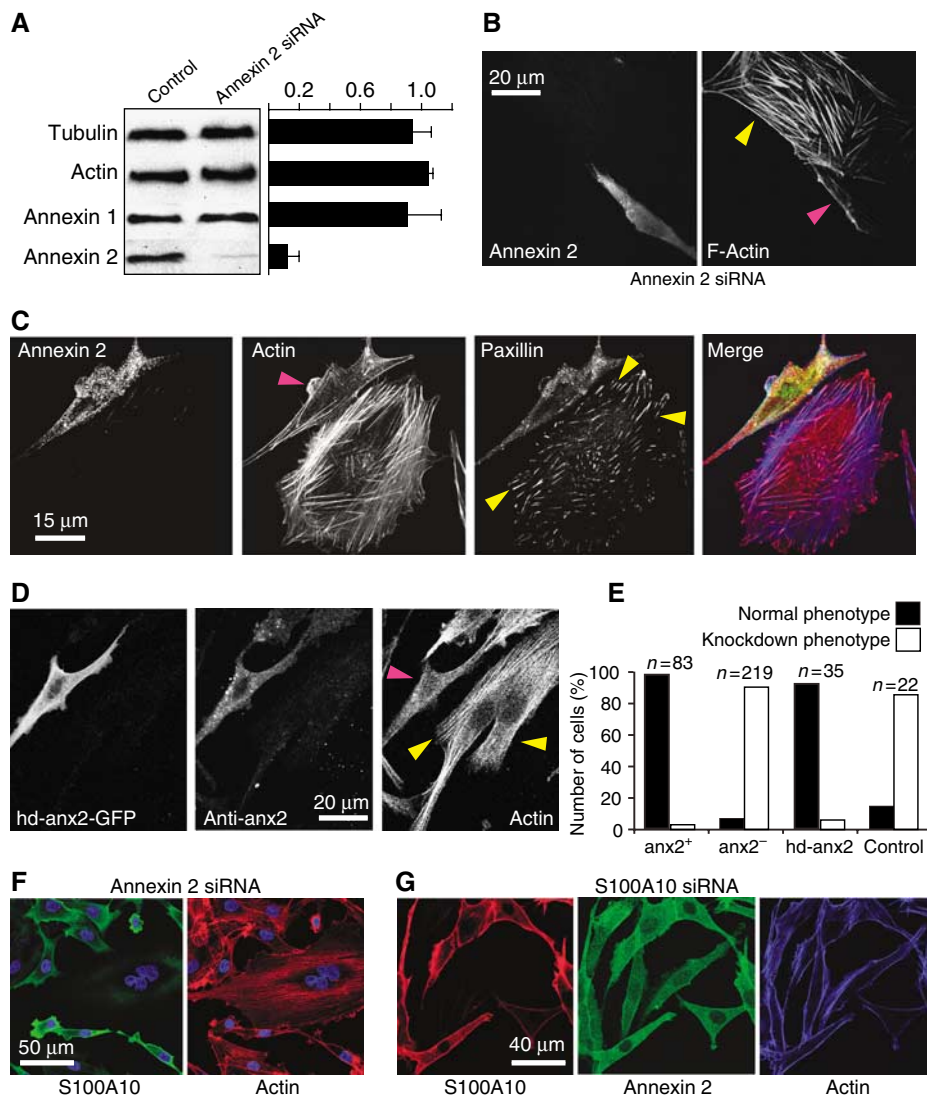


Figure 2 Loss of annexin 2 leads to reconfiguration of the actin cytoskeleton. (A) Cells were treated with siRNA for annexin 2 and extracts were analysed by Western blotting. Following 4 days of exposure to siRNA, annexin 2 levels were depressed, whereas α -tubulin, actin and annexin 1 were unaffected. The histogram shows protein levels, as judged by densitometric scanning, in siRNA-treated cells relative to those in control cells ($n = 3$). (B) The panels show two MIO cells cultured in the presence of annexin 2 siRNA, one of which is depleted of annexin 2 (yellow arrowhead). TRITC-phalloidin staining reveals reorganisation of F-actin into prominent stress fibres in the cell lacking annexin 2. (C) MIO cells were treated with siRNA for annexin 2 and triple stained for annexin 2, F-actin and paxillin. The lower of the two cells shows the accumulation of actin stress fibres in the absence of annexin 2 (as in (B)), with paxillin positive structures at fibre ends consistent with the formation of focal adhesions (yellow arrowheads). Annexin 2 depleted cells also lacked the actin-rich ruffles observed in control cells (pink arrowhead). (D) MIO cells were depleted of annexin 2 for 3 days as in (B), then transfected with either an hd-anx2-GFP vector or GFP alone. Cells were fixed 24 h after transfection and stained with phalloidin and antisera to annexin 2. The panels show a field of cells depleted of annexin 2, in which the cell marked by the pink arrowhead expresses hd-anx2-GFP and has a normal phenotype, whereas the neighbouring cells (yellow arrowheads) display the knockdown phenotype. (E) The relationship between cellular F-actin phenotype and annexin 2 expression was quantified by counting cells in multiple fields of cells such as those represented in (D). The columns labelled 'anx2⁺' and 'anx2⁻' show the percentages of cells displaying normal and knockdown phenotypes following exposure to annexin 2 siRNA. The columns labelled 'hd-anx2' and 'control' show comparable data from siRNA-treated cells subsequently transfected with hd-anx2-GFP and GFP, respectively. (F) MIO cells were depleted of annexin 2 as in (B), and then immunostained for S100A10 and F-actin. Nuclei were counter-stained with DAPI. Cells lacking annexin 2, characterised by their F-actin phenotype, also exhibited a reduction in staining for S100A10. (G) MIO cells were depleted of S100A10 using specific siRNA oligonucleotides, then immunostained for S100A10, annexin 2 and F-actin. Cells lacking S100A10 exhibited normal levels of annexin 2 and had an unchanged F-actin phenotype.

These results show that maintenance of a normal actin phenotype requires annexin 2 but not S100A10.

Annexin 2 knockdown alters cell shape and protrusive activity

To examine the effects of loss of annexin 2 in living cells, spontaneous protrusive activity was monitored in control and

annexin 2-depleted cells over an approximately 20-min period (Figures 3A and B; see also Supplementary data, movies 1 and 2). Quantitative analysis of stills from these movies revealed that the overall size of the cell footprint changed little throughout the experiment, regardless of whether or not cells were depleted of annexin 2 (Figures 3C and D). Since annexin 2-depleted cells also appeared to undergo fewer

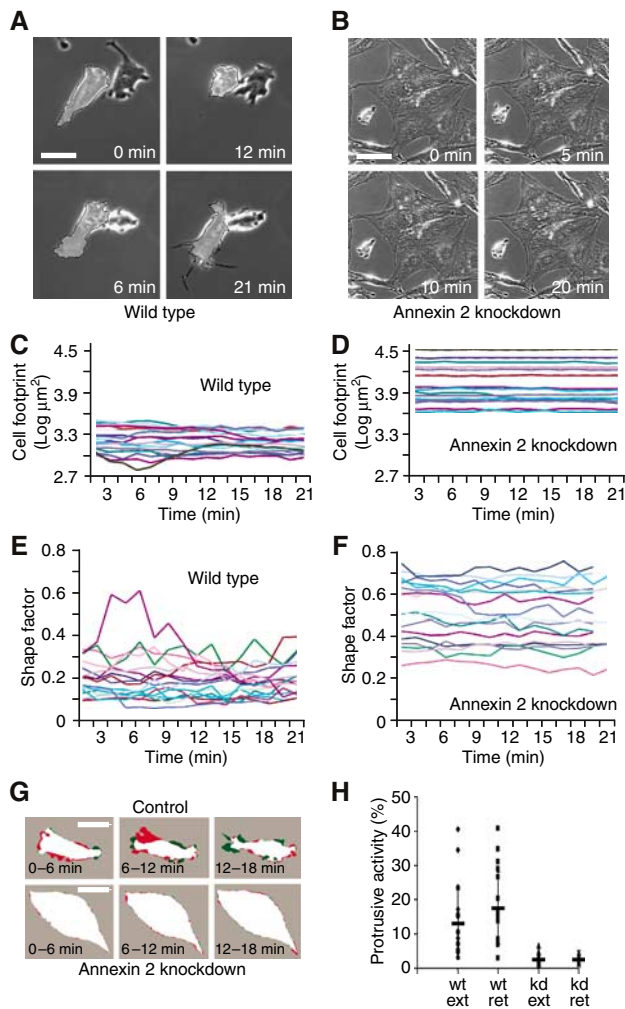


Figure 3 Annexin 2 is required for changes in cell shape. (A, B) MIO cells were cultured in the presence of siRNA for annexin 2 prior to video timelapse recording of spontaneous shape changes. See Supplementary data, Movies 1 and 2. Scale bar in A = 10 μm . Scale bar in B = 30 μm . (C, D) Wild type and annexin 2 knockdown cells were readily distinguished on the basis of size, since loss of annexin 2 led to an increase in cell footprint of approximately one order of magnitude (see Figure 2). The graphs show that cells exhibited only modest changes in footprint during the experiment. (E, F) The Shapefactor of large, annexin 2 depleted cells remained fairly constant over a 20-min period, but that of control cells oscillated as the cells extended and retracted actin-rich ruffles. The variances of cellular footprint and Shapefactor for knockdown and control cells were compared by the F-test and are 2.06E-07 and 8.84E-46, respectively. The graphs show data collected from 17 individual cells where each coloured trace represents one cell. (G) The cell footprint of annexin 2-depleted (scale bar = 30 μm) and control (scale bar = 10 μm) MIO cells was circumscribed from frames of time-lapse videos of live cells. Frames 6 min apart were superimposed and the proportion of the footprint of the cell that had extended (green) or retracted (red) between frames was calculated using Metamorph. These regions represent dynamic plasma membrane ruffles driven by rapid underlying actin polymerisation and depolymerisation. (H) Data are expressed as percentage extension/retraction of total cell footprint. Percentage retraction and extension were calculated by measuring the decrease or increase in cell footprint at 12 min when compared against the cell footprint at 6 min. Each dot on the scattergram represents a single cell. Wild type (wt) cells both extended (ext) and retracted (ret) a greater proportion of their cell footprint than did annexin 2 knockdown (kd) cells in any 6 min period.

shape changes, we analysed the same cohort of cells using the Shapefactor algorithm in Metamorph. This measures the deviation of a given form from a circle (which has unit value on the scale). The more elongated or irregular the form, the lower the Shapefactor value. Wild-type (wt) cells tended to have lower Shapefactor values than annexin 2-depleted cells (Figures 3E and F), indicating that loss of annexin 2 leads to fewer protrusions and invaginations, and hence a more rounded profile. Although both cell populations exhibited changes in Shapefactor during the experiment, these were significantly less marked in annexin 2-depleted cells than in wt cells, as judged by F-test analysis (wt = 2.06E-07 and knockdown = 8.84E-46). We also analysed protrusion dynamics by quantifying lamellipod extension and retraction (Bailey *et al*, 1998) in control and annexin 2-depleted cells (Figures 3G and H). The results show that when measured relative to cell area, extension and retraction of lamellipodia are significantly greater in control than annexin 2-knockdown cells. Collectively, these data show that loss of annexin 2 leads to diminished plasticity of the actin cytoskeleton and a reduction in dynamic actin-based structures such as lamellipodia and ruffles.

Annexin 2 binds G-actin and inhibits actin polymerisation

Although annexin 2 has been shown to bundle preformed actin filaments in the presence of millimolar calcium *in vitro* (Glenny, 1987), our observation that annexin 2 is preferentially associated with actin at sites of cytoskeletal remodelling prompted us to examine whether annexin 2 has a more direct role in the regulation of actin dynamics. To determine whether annexin 2 physically interacts with actin *in vivo*, we first examined fluorescence resonance energy transfer (FRET) between annexin 2-CFP and YFP-actin. We performed acceptor photobleaching experiments in which the CFP image was recorded before and after bleaching of YFP in selected regions of interest (Figures 4A and B). In control experiments utilising YFP-actin with CFP no FRET was observed, whereas FRET at an approximate average efficiency of >40% was observed in cells co-expressing YFP-actin and annexin 2-CFP. Although FRET was evident between annexin 2 and actin at ruffles, it was also apparent throughout the cell, indicating that annexin 2 and actin may exist in close physical proximity both in the cytosol and at the plasma membrane. To test the generality of this observation we performed identical FRET experiments in two other cell lines, A431 squamous carcinoma cells and B16F10 melanoma cells, and obtained similar results with comparable FRET efficiency values (Supplementary Figure 4). In a further set of experiments we examined whether or not the strength of the FRET signal between annexin 2-CFP and YFP-actin might be influenced by the concentration of intracellular Ca^{2+} ($[\text{Ca}^{2+}]_i$). A431 cells preloaded with BAPTA-AM to reduce $[\text{Ca}^{2+}]_i$ exhibited a significant reduction in FRET efficiency when compared to control cells, whereas elevation of $[\text{Ca}^{2+}]_i$ stimulated by the addition of ionomycin had the opposite effect (Figure 4C), suggesting that the interaction between annexin 2 and actin is Ca^{2+} -dependent.

The possibility of a physical interaction between annexin 2 and actin suggested that annexin 2 might directly influence actin polymerisation/depolymerisation. To test this, we investigated the effect of annexin 2 on the rate of spontaneous

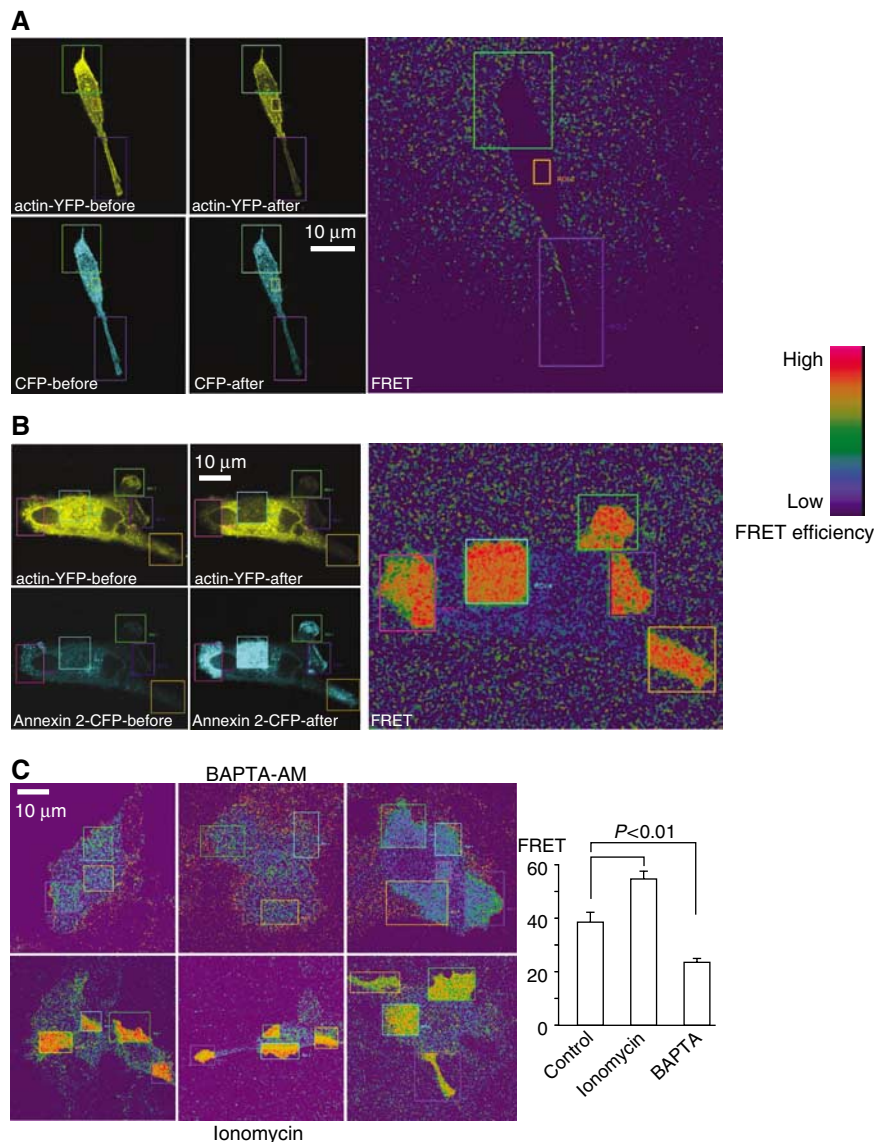


Figure 4 FRET analysis of annexin 2 and actin. **(A)** MIO cells were co-transfected with YFP-actin and CFP, then fixed and analysed by confocal microscopy after 24 h. CFP and YFP emission signals were captured before and after 50% photobleaching YFP. FRET is indicated as the relative increase in CFP emission following YFP photobleaching, where the scale bar represents high FRET efficiency with bright colours (red). In this control experiment, there was no measurable FRET between YFP-actin and CFP. **(B)** MIO cells were transfected with YFP-actin and annexin 2-CFP and subjected to image analysis as described in (A). A significant increase in CFP fluorescence was observed following YFP photobleaching equivalent to an average FRET efficiency of ~40%. Similar experiments in A431 and B16F10 cells also yielded FRET measurements of up to 40% (see Supplementary data). These data indicate that FRET occurs between annexin 2-CFP and YFP-actin, corresponding to a physical proximity of the two fluorophores of <8 nm. **(C)** FRET experiments were performed in cells immediately following either chelation of intracellular Ca^{2+} [Ca^{2+}]_i using BAPTA-AM (top three panels) or elevation of [Ca^{2+}]_i using ionomycin (bottom three panels). The histogram shows that the average FRET intensity is increased when Ca_i^{2+} is raised and diminished when Ca_i^{2+} is reduced ($n = 20$ for each sample).

actin polymerisation *in vitro*. In kinetic measurements of fluorescence intensity in an assay employing pyrene-labelled ATP-actin monomers, recombinant annexin 2 inhibited the rate of polymerisation of Mg^{2+} -ATP G-actin monomers in the presence of 50 μM Ca^{2+} in a dose-dependent manner. The inhibitory effect of 5 μM annexin 2 was completely abolished in the presence of 1 mM EGTA (Figures 5A and B). In contrast, annexin 5 had no effect in this assay (not shown), suggesting that unlike other common activities of these proteins, inhibition of actin polymerisation is not a generic annexin property. On close examination we noticed an increase in the lag-time associated with the formation of actin nuclei at the commencement of polymerisation in

the presence of annexin 2 (Figure 5A inset), a significant annexin 2-dependent reduction in the rate of actin polymerisation, and (not shown) a minor reduction in the final concentration of F-actin filaments attained as polymerisation plateaued. This is consistent with annexin 2 having the capacity to bind both monomeric G-actin (suppressing filament nucleation by monomer sequestration, and sequestering a pool of G-actin from incorporation into filaments at the end of the experiment) and to interfere with filament elongation. In agreement with these observations, a quantitative morphometric analysis of actin filaments prepared in the absence and presence of equimolar annexin 2 (Figures 5C-E) showed that annexin 2 shifts the profile

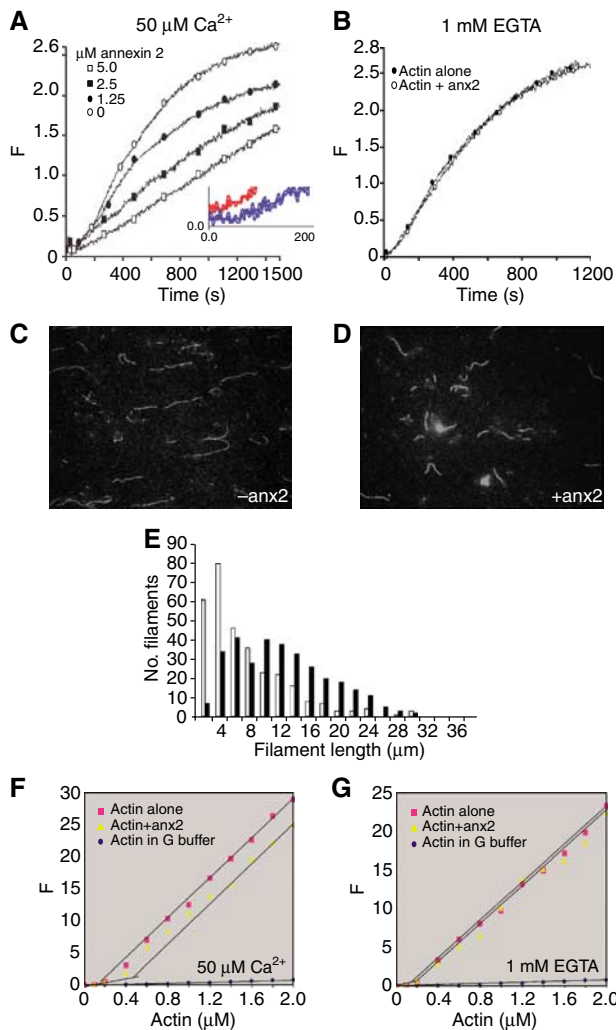


Figure 5 Annexin 2 is a G-actin binding protein. (A, B) Effect of annexin 2 on spontaneous actin polymerisation in the presence of (A) $50 \mu\text{M Ca}^{2+}$ or (B) 1 mM EGTA . The inset shows a increased lag phase in presence of annexin 2 (blue) compared to the control without annexin 2 (red). (C–E) F-actin filaments (10% rhodamine-labelled Mg^{2+} -ATP) assembled in the presence of annexin 2 are shorter. The histogram (E) represents the distribution of filament lengths observed after G- Mg^{2+} -ATP actin was allowed to polymerise for 2 h (>200 filaments were measured, the histogram shows one experiment from three independent assays, representative images of which are shown in C, D). Filament length was calculated using Metamorph. (F, G) Effects of annexin 2 on actin polymerisation at steady state. Inclusion of annexin 2 in the polymerisation mix shifts the critical concentration plot of actin assembly in a calcium-dependent manner. Annexin 2 ($2 \mu\text{M}$) was incubated with increasing concentrations of actin in the presence of $50 \mu\text{M Ca}^{2+}$ (F) or 1 mM EGTA (G).

of actin filament length towards shorter filaments. Annexin 2 ($2 \mu\text{M}$) also Ca^{2+} -dependently increased the apparent critical concentration for actin polymerisation measured at steady state from 0.13 to $0.45 \mu\text{M}$, providing further evidence that annexin 2 can bind and sequester actin monomers. The K_d of annexin 2 for actin monomers estimated from the results is around $0.7 \mu\text{M}$, a value similar to that of other monomer-sequestering proteins such as profilin (Figures 5F and G).

Kinetic measurements were performed to evaluate the effects of annexin 2 on the assembly and disassembly of

actin at the barbed and pointed-ends of actin filaments. Annexin 2 dramatically inhibited the polymerisation of actin filaments in a dose-dependent manner when actin assembly was initiated by spectrin seeds, that is, when the pointed-ends were blocked (Figure 6A). Conversely, a range of concentrations of annexin 2 up to $5 \mu\text{M}$ had little effect on actin assembly when the barbed ends were blocked with gelsolin (Figure 6B). In this case, we observed only a slight reduction in the final concentration of F-actin that polymerised as the reaction plateaued. Thus, annexin 2 may be able to sequester a small pool of G-actin but does not appear to be able to block polymerisation at the pointed-end of the filament. Representation of the effect of annexin 2 as a function of elongation rate reveals that the concentration of annexin 2 required for half-maximal inhibition of barbed end polymerisation is approximately 125 nM (Figure 6C). Furthermore, annexin 2 also decreased the depolymerisation rate of preformed actin filaments in a dose-dependent manner (Figure 6D). This is consistent with annexin 2 capping the fast depolymerising barbed ends of the filaments, allowing dissociation only from the slowly depolymerising pointed ends.

Annexin 2 requires free barbed ends for targeting to ruffles

To determine whether annexin 2 requires free barbed-ends to localise to membrane ruffles *in vivo*, we used the approach of Bear *et al* (2002), who reported that low concentrations of cytochalasin D (CD) can be used to effectively block the barbed ends of actin filaments without significant disruption of the filamentous actin cytoskeleton. We found that in control cells Wave-1 (which is not localised to ruffles by a direct interaction with actin barbed-ends) was insensitive to concentrations of CD $<100 \text{ nM}$, and that it co-localised with annexin 2 to actin-rich membrane ruffles (Figure 7A). In contrast, annexin 2 was completely displaced from membrane ruffles following the addition of 40 nM CD to culture medium, whereas the actin cytoskeleton and Wave-1 were unaffected. In control experiments, a range of concentrations of Latrunculin B (LatB) up to 100 nM did not diminish the co-localisation of Wave-1, annexin 2 and actin at membrane ruffles. Interestingly, the lowest concentration of CD (40 nM) effective in displacing annexin 2 from membrane ruffles was also sufficient to partially reverse the F-actin phenotype in siRNA-treated cells lacking annexin 2 (Figure 7B). The flattened cells became more elongated together with redistribution of F-actin from stress fibres to the cortex. This pharmacomimetic reversal of phenotype was however only partial and there was little evidence of an increase in cellular ruffling. In similar experiments, LatB had no effect on the actin phenotype, suggesting that the knockdown phenotype was not the result of diminished sequestration of monomeric G-actin. These observations show that annexin 2 requires free barbed-ends of actin filaments to localise to membrane ruffles, and indicate that the potential capping activity of annexin 2 can be at least partially complemented by the capping activity of CD but not by the actin sequestering activity of LatB. Using rhodamine-labelled actin to report the presence of free barbed ends in partially permeabilised cells (Chan *et al*, 1998), we were also able to co-localise annexin 2 (by indirect immunofluorescence) with the barbed-ends of actin filaments in MIO cell ruffles and the

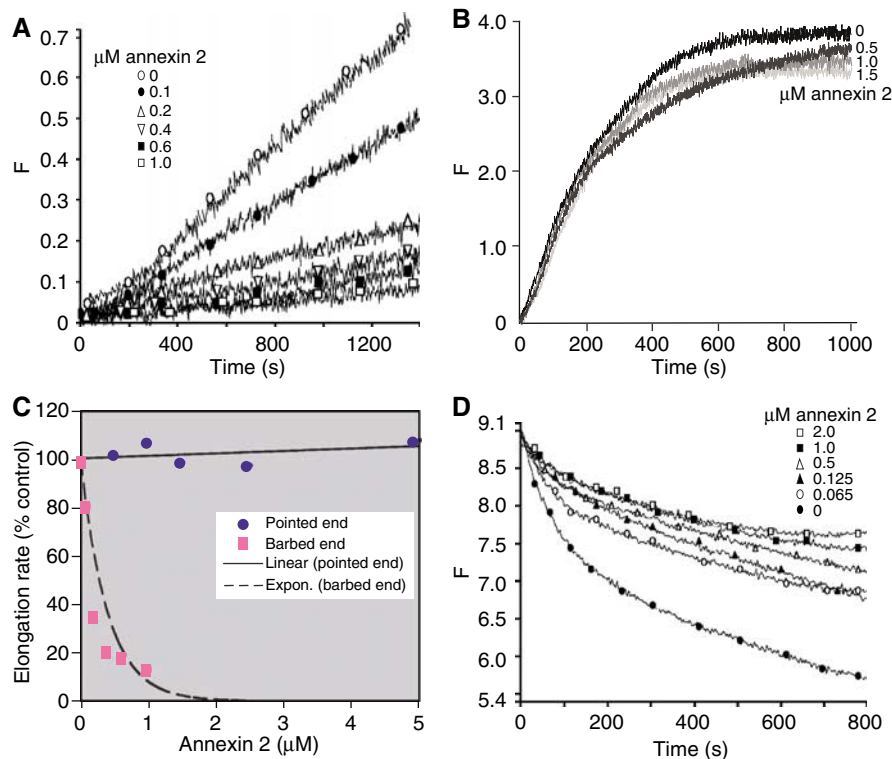


Figure 6 Annexin 2 is a barbed end capping protein. (A) Spectrin seeds were preincubated with increasing concentrations of annexin 2. The rate of polymerisation of 0.45 μM actin in the presence of these seeds is inversely proportional to the concentration of annexin 2. This is consistent with inhibition of polymerisation at the barbed-end when the pointed-end of the growing filament is blocked by spectrin. (B) In the reciprocal experiment in which annexin 2 was preincubated with gelsolin seeds, which blocks the barbed-end, there was little effect of annexin 2 on the rate of polymerisation of 2 μM actin. This shows that annexin 2 does not have the capacity to block polymerisation at the slowly elongating pointed end of the growing filament. The slight reduction in the 'equilibrium' concentration of F-actin could be due to G-actin sequestration by annexin 2. (C) Annexin 2 participates in filament growth at the barbed-end and not the pointed-end. Annexin 2 shows concentration dependent inhibition of F-actin filament elongation when the pointed-ends of the filaments are blocked with spectrin seeds (red squares). There is no additional effect on polymerisation when the barbed ends are blocked with gelsolin (blue circles). (D) Kinetics of depolymerisation of 100 nM actin filaments in the presence of increasing concentration of annexin 2.

EGF-induced ruffles of MTLn3 cells (Figure 7C). These observations confirm that annexin 2 is well placed to modulate actin polymerisation by localising to a cellular environment enriched in free barbed ends and close to the plasma membrane.

Discussion

The ability of annexin 2 to bind and bundle polymerised actin in the presence of millimolar calcium *in vitro* is well established, and an F-actin-binding domain has been assigned to its C-terminus (Jones *et al*, 1992; Filipenko and Waisman, 2001). Interestingly, other annexins with this conserved C-terminus do not exhibit actin-bundling activity, and in cells only a very small proportion of annexin 2 appears to associate with actin bundles in stress-fibres or microvilli. Indeed, annexin 2 is more frequently associated with dynamic membrane-cytoskeletal structures such as rocketing macropinosomes (Merrifield *et al*, 2001), phagosomes (Sakai *et al*, 2001) and the actin pedestals of enteropathogenic *Escherichia coli* (Zobiack *et al*, 2002). In this study, we localised annexin 2 to the membrane ruffles of MIO cells and spreading MTLn3 cells. Time-lapse imaging showed enrichment of annexin 2 in ruffles whereas quiescent cytoplasmic protrusions were devoid of

annexin 2. FRET between annexin 2-CFP and YFP-actin revealed that annexin 2 associates Ca^{2+} -dependently with actin both in the cytoplasm and within these dynamic ruffling structures.

The critical concentration experiments and the increased lag-time required for spontaneous actin polymerisation suggest that annexin 2 can bind and sequester G-actin. Many proteins have been reported to bind to monomeric actin in the cytoplasm (Paavilainen *et al*, 2004), including the thymosin family, profilin, cofilin and gelsolin. If annexin 2 behaves in a similar manner to other monomer-binding proteins, it would have the additional functionality that it can also bind directly to the plasma membrane. Thus, it has the potential to deliver actin monomers directly to the cell cortex where they might be required for rapid polymerisation. There are several ways in which this process could be regulated; by complex formation with its binding partner S100A10, by phosphorylation by protein kinase C or c-src, or by phosphatidylinositol 4,5-bisphosphate (Hayes *et al*, 2004a, b; Rescher *et al*, 2004). Experiments in which we overexpressed annexin 2-CFP and YFP-actin and measured FRET between them, support the idea that the two molecules can interact *in vivo*. However, this technique cannot distinguish the interaction between annexin 2 and G-actin monomers with an interaction with the ends of short F-actin

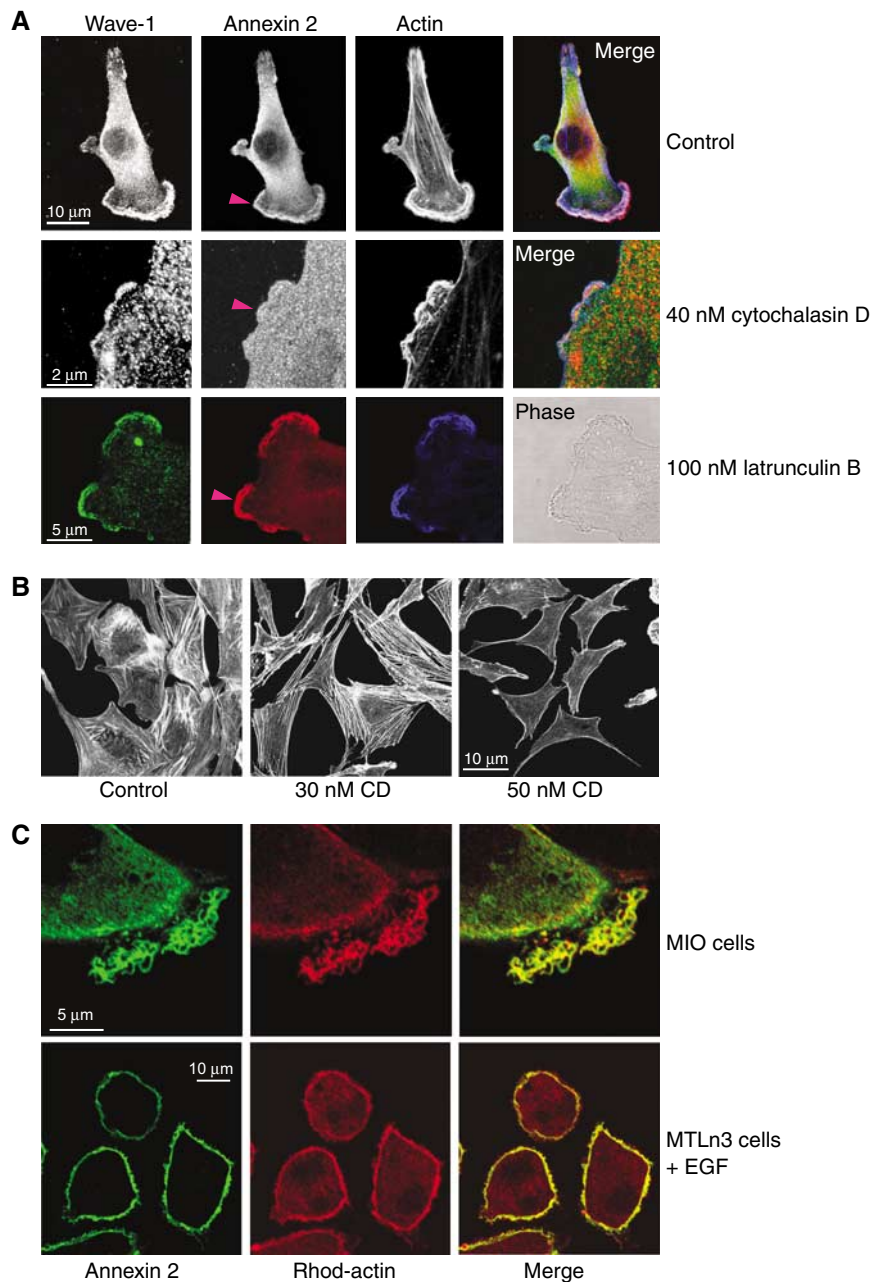


Figure 7 Cytochalasin D displaces annexin 2 from membrane ruffles. (A) MIO cells were cultured overnight in the presence or absence of 40 nM Cytochalasin D prior to fixing and immunostaining for annexin 2, Wave-1 and F-actin. Under these conditions, annexin 2 was almost completely displaced from actin-rich ruffles (pink arrowheads) whereas Wave-1 and the F-actin ruffles were unaffected. In contrast, 100 nM Latrunculin B had no effect on the localisation of annexin 2. These data show that the association of annexin 2 with the barbed-ends of actin filaments mediates its localisation to ruffles. (B) Annexin 2 was knocked down using siRNA over a 4-day period. Cells demonstrate loss of cortical actin, loss of ruffles, a flattened morphology and accumulation of thickened stress fibres. Overnight incubation with 0, 30 and 50 nM cytochalasin D revealed partial reversal of the knockdown phenotype at the highest concentration used. (C) Annexin 2 colocalises with the barbed-ends of F-actin filaments in MIO cell ruffles and EGF-induced ruffles of MTLn3 cells. Barbed-ends were labelled by incorporation of rhodamine-actin into partially permeabilised cells and subsequent immunofluorescent labelling of annexin 2.

filaments. Annexin 2 co-localised with the barbed-ends of actin filaments in the dynamic ruffles of MIO cells and the EGF-induced ruffles of MTLn3 cells, suggesting it is well placed to act as a barbed-end capping protein. In future work, it will be of interest to determine whether physiological Ca^{2+} agonists drive annexin 2-actin FRET at sites such as ruffles. Capping proteins such as CP or CapG also bind monomeric actin, but have the highest affinity for the barbed-ends of F-actin filaments where the actin monomers

have a particularly receptive conformation. *In vitro* biochemical assays showed that while annexin 2 can inhibit polymerisation at the barbed-ends of F-actin filaments, it has almost no effect on polymerisation at the pointed-ends. Annexin 2 also inhibited actin depolymerisation, and incubation of growing F-actin filaments with annexin 2 resulted in the formation of shorter filaments. The importance of the availability of barbed-ends and the maintenance of a pool of short F-actin filaments is an established concept in actin

dynamics (Carlier, 1998; Borisy and Svitkina, 2000; Cooper and Schafer, 2000). Capping proteins have critical roles in actin dynamics, and depletion of CP using shRNA in motile cell lines has been shown to lead to loss of cellular ruffles and their substitution with ENA-dependent filopodia (Mejillano *et al*, 2004). Consistent with such observations, we show here that depletion of annexin 2 in MIO cells leads to the loss of dynamic actin structures. Other studies reporting depletion of annexin 2 using siRNA have not specifically addressed issues of actin dynamics (e.g. Mayran *et al*, 2003), although one recent report identified annexin 2 as the target of withaferin A, a naturally occurring antiproliferative steroidal lactone, that promotes the disruption of the actin cytoskeleton by binding to and modulating the properties of annexin 2 (Falsey *et al*, 2006). In contrast, we show here that cells depleted of annexin 2 become enriched in stress fibres and show a relative reduction in their cortical actin. The stress-fibres terminated in extended focal adhesions as evidenced by paxillin staining, suggesting that rather than generating an abnormal actin phenotype, loss of annexin 2 switches cells from a dynamic, ruffling physiology to a relatively quiescent, stress-fibre dominated physiology. The fact that CD at low concentrations could partially reverse this phenotype, whereas LatB could not, further supports the idea that annexin 2 has barbed-end capping activity, and that it is this rather than G-actin binding that dominates this change in phenotype.

Our results do not rule out an ancillary role for annexin 2, in which it competes with other capping proteins (perhaps in a Ca^{2+} -dependent way) to expose barbed-ends in the vicinity of the plasma membrane. The formation of actin networks is dependent upon many factors such as the Arp2/3 complex (Higgs and Pollard, 2001; Pollard and Borisy, 2003) and actin-binding proteins such as Wasp, Wave and Scar. These proteins are themselves regulated by a number of small GTPases including Rho, Rac1 and Cdc42. Annexin 2 has been purified in complexes containing Rac1 at the site of actin-rich cell-cell contacts (Hansen *et al*, 2002), and associates with AHNAK at the cytosolic surface of the plasma membrane of cell-cell contacts in MDCK cells (Benaud *et al*, 2004). Downregulation of annexin 2 or S100A10 inhibits localisation of AHNAK to these structures. AHNAK is thought to organise the actin cytoskeleton by its interaction with rho-family kinases. Thus, annexin 2 may be capable of modulating actin dynamics by acting as a scaffold for the assembly of actin-rich complexes at membranes. The fact that CD can displace annexin 2 from ruffles while partially reverting the phenotype in knockdown cells suggests that annexin 2 might well be involved in such a process.

In summary, we have demonstrated that annexin 2 can regulate actin filament turnover, most likely through monomer sequestration and barbed-end capping activities. Although these activities are shared in part by other actin-binding proteins such as profilin, thymosin beta 4 and capping proteins, the abundance of annexin 2 in many cell types implicates it as a significant player in the regulation of actin filament dynamics. Our findings provide new insight into annexin 2 function, which may not only explain the essential requirement for annexin 2 in the actin-dependent movement of macropinosomes (Merrifield *et al*, 2001) but also suggest a broader role for annexin 2 as a modulator of actin dynamics *in vivo*.

Materials and methods

Protein preparation

Actin was purified from rabbit muscle (Spudich and Watt, 1971) and rhodamine-labelled as previously described (Chan *et al*, 1998). Spectrin was isolated from human erythrocytes (North London Hospital Service) and spectrin-actin seeds were made as previously described (Casella *et al*, 1995). Gelsolin (Sigma) seeds and porcine profilin were made as described elsewhere (Blanchoin *et al*, 2000). Rat annexin 2 (gift from Dr J Ayala-Sanmartin) was expressed and purified from yeast (Ayala-Sanmartin *et al*, 2000). Pyrene actin was purchased from Cytoskeleton.

Polymerisation assays

Actin (2 μM , 5% pyrenyl labelled) was polymerised in 5 mM Tris-HCl at pH 8.0, 50 mM KCl, 1 mM MgCl_2 , 0.2 mM ATP in the presence of 50 μM CaCl_2 or 1 mM EGTA and in the presence or absence of annexin 2 at indicated concentrations. Fluorescence changes were recorded as a function of time on a fluorescence spectrometer (Perkin-Elmer). For steady-state polymerisation assays various concentrations of actin (10% pyrenyl-labelled) were allowed to polymerise in 5 mM Tris-HCl at pH 8.0, 50 mM KCl, 1 mM MgCl_2 , 0.2 mM ATP in the presence of 50 μM CaCl_2 or 1 mM EGTA and in the presence or absence of 2 μM annexin 2 at RT overnight. Critical concentrations (cc) were calculated from the intercept of two linear regressions fitted to the data. The apparent dissociation constant (K_d) for the annexin 2-G actin complex was calculated using the formula:

$$K_d = (T - \text{TA})(A_0)/\text{TA}$$

where T is the total annexin 2 concentration, A_0 is the critical concentration of actin alone, and TA is the concentration of annexin 2-actin complex, defined as the difference between the steady-state F-actin concentration without annexin 2 to that with annexin 2.

Barbed end and pointed end elongation

Rates of filament growth from the pointed or barbed ends were measured by adding 2 μM actin (10% pyrenyl labelled) to gelsolin seeds, or 0.45 μM actin (10% pyrenyl labelled) to spectrin seeds, in 5 mM Tris-HCl at pH 8.0, 50 mM KCl, 1 mM MgCl_2 , 0.2 mM ATP, 50 μM CaCl_2 in the presence or absence of annexin 2 at indicated concentrations.

Depolymerisation

Actin (10 μM , 50% pyrenyl labelled) was polymerised in 5 mM Tris-HCl at pH 8.0, 50 mM KCl, 1 mM MgCl_2 , 0.2 mM ATP, 50 μM CaCl_2 (F-buffer) at 4°C overnight. Various concentrations (final) of annexin 2 as indicated were added to F-actin 2 min before it was diluted to 100 nM with F-buffer.

Fluorescence microscopy of actin filaments

Actin (5 μM , 10% rhodamine-labelled) was polymerised in F-buffer in the presence or absence of 5 μM annexin 2 at RT for 2 h. Samples were diluted 100-fold in F-buffer containing 1% β -mercaptoethanol and 0.5 μM phalloidin, and loaded onto a nitrocellulose coated coverslip. Images were captured using an inverted epifluorescence microscope (Zeiss-Axiovert 100M connected to an Openlab-driven acquisition system (Improvision)) and filament lengths were measured by analysis of TIFF images using Metamorph.

siRNA experiments

siRNA oligonucleotides with specificity for annexin 2 were obtained from Dharmacon (AACCGGUUCAGUGCAUUCAG and AAGUGC AUAUGGGUCUGUCA). Subconfluent MIO Müller cells were transiently transfected with the oligonucleotides using Oligofectamine (Invitrogen). In our hands, although each siRNA worked moderately well and equally efficiently alone, a combination of the two oligos worked better than either independently. Efficient knockdown of annexin 2 required at least 3 days. Those for human S100A10 were obtained from Qiagen (AAAGGAGGACCUGAGAGUA CU). Control experiments used oligofectamine alone or nonspecific oligonucleotides. For phenotype reversal experiments, site-directed mutagenesis was used to introduce three conservative changes into the annexin 2-GFP expression vector at the siRNA target site (AACCGGUUCAGUGC changed to AAUCUGUCCAGUGU). The resulting siRNA-hardened construct we refer to as hd-anx2-GFP.

Coverslips on which endogenous annexin 2 had been knocked down in at least 90% of cells for 3 days were transiently transfected with hd-annx2-GFP and after 48 h the cells were fixed and stained for annexin 2 with the monoclonal antibody HH7 (a kind gift of V Gerke) with a Cy3 secondary antibody, and F-actin (Alexa-660 phalloidicin). Images were captured of representative fields of cells, and the number of green (hd-annx2-GFP) cells that exhibited the wildtype or annexin 2 knockdown phenotype, as well as those that were annexin 2 positive or negative was counted.

Measurement of protrusive activity

To quantify the change in cellular footprint associated with annexin 2 depletion, MIO cells were exposed to annexin 2 siRNA as described above, then fixed and stained for annexin 2 and F-actin using the monoclonal antibody HH7 and TRITC-phalloidin (Molecular Probes), respectively. High-resolution images of cells were captured using a BioRad confocal microscope. The respective cellular 'footprints' of annexin positive and annexin negative cells were obtained by manually drawing round the cells and calculating the surface areas thus circumscribed using Metamorph. To assess protrusive activity phase-contrast time-lapse images were captured of spontaneous shape changes in MIO cells treated with annexin 2 siRNA or a control siRNA (specific for annexin 5, but which has no effect on levels of annexin 5 protein or mRNA). Images were captured every 30 s, and processed in Metamorph to calculate the footprint and Shapefactor of individual cells. Shapefactor provides information as to cell shape dynamics, and is denoted by the formula $4\pi r/p^2$, where p is the perimeter of the circumscribed cell. Cells with a near circular footprint have a Shapefactor value close to 1, whereas cells with extended filopodia or ruffles have Shapefactors closer to 0.

FRET experiments

Human MIO cells, B16F10 melanoma cells or A431 cells were co-transfected with annexin 2-CFP and actin-YFP, or CFP and actin-YFP, using Lipofectamine 2000 (Invitrogen). After 24 h (A431) or 48 h (MIO cells and B16F10s) cells were fixed with 4% paraformaldehyde and imaged using a Leica confocal microscope. Ionomycin was added to a final concentration of 10 μ M for 30 min. Cells were loaded with 5 μ M BAPTA-AM for 30 min. FRET was measured by the method of acceptor bleaching and quantified by Leica LCS software.

References

- Ali SM, Geisow MJ, Burgoyne RD (1989) A role for calpactin in calcium-dependent exocytosis in adrenal chromaffin cells. *Nature* **340**: 313–315
- Ayala-Sanmartin J, Gouache P, Henry JP (2000) N-terminal domain of annexin 2 regulates Ca(2+)-dependent membrane aggregation by the core domain: a site directed mutagenesis study. *Biochemistry* **39**: 15190–15198
- Babiychuk EB, Draeger A (2000) Annexins in cell membrane dynamics* Ca(2+)-regulated association of lipid microdomains. *J Cell Biol* **150**: 1113–1124
- Bailly M, Yan L, Whitesides GM, Condeelis JS, Segall JE (1998) Regulation of protrusion shape and adhesion to the substratum during chemotactic responses of mammalian carcinoma cells. *Exp Cell Res* **241**: 285–299
- Bear JE, Svitkina TM, Krause M, Schafer DA, Loureiro JJ, Strasser GA, Maly IV, Chaga OY, Cooper JA, Borisy GG, Gertler FB (2002) Antagonism between Ena/VASP proteins and actin filament capping regulates fibroblast motility. *Cell* **109**: 509–521
- Benaud C, Gentil BJ, Assard N, Court M, Garin J, Delphin C, Baudier J (2004) AHNAK interaction with the annexin 2/S100A10 complex regulates cell membrane cytoarchitecture. *J Cell Biol* **164**: 133–144
- Blanchoin L, Pollard TD, Mullins RD (2000) Interactions of ADF/cofilin, Arp2/3 complex, capping protein and profilin in remodeling of branched actin filament networks. *Curr Biol* **10**: 1273–1282
- Borisy GG, Svitkina TM (2000) Actin machinery: pushing the envelope. *Curr Opin Cell Biol* **12**: 104–112
- Carlier MF (1998) Control of actin dynamics. *Curr Opin Cell Biol* **10**: 45–51
- Casella JF, Barron-Casella EA, Torres MA (1995) Quantitation of Cap Z in conventional actin preparations and methods for further purification of actin. *Cell Motil Cytoskeleton* **30**: 164–170
- Chan AY, Raft S, Bailly M, Wyckoff JB, Segall JE, Condeelis JS (1998) EGF stimulates an increase in actin nucleation and filament number at the leading edge of the lamellipod in mammary adenocarcinoma cells. *J Cell Sci* **111**: 199–211
- Cooper JA, Schafer DA (2000) Control of actin assembly and disassembly at filament ends. *Curr Opin Cell Biol* **12**: 97–103
- Diakonova M, Gerke V, Ernst J, Liautard JP, van der Vusse G, Griffiths G (1997) Localization of five annexins in J774 macrophages and on isolated phagosomes. *J Cell Sci* **110**: 1199–1213
- Drust DS, Creutz CE (1988) Aggregation of chromaffin granules by calpactin at micromolar levels of calcium. *Nature* **331**: 88–91
- Emans N, Gorvel JP, Walter C, Gerke V, Kellner R, Griffiths G, Gruenberg J (1993) Annexin II is a major component of fusogenic endosomal vesicles. *J Cell Biol* **120**: 1357–1369
- Falsey RR, Marron MT, Gunaherath GM, Shirahatti N, Mahadevan D, Gunatilaka AA, Whitesell L (2006) Actin microfilament aggregation induced by withaferin A is mediated by annexin II. *Nat Chem Biol* **2**: 33–38
- Filipenko NR, Waisman DM (2001) The C terminus of annexin II mediates binding to F-actin. *J Biol Chem* **276**: 5310–5315
- Gerke V, Creutz CE, Moss SE (2005) Annexins: linking calcium signaling to membrane function. *Nat Rev Mol Cell Biol* **6**: 449–461
- Glennay Jr JR (1987) Calpactins: Calcium-regulated membrane-skeletal proteins. *Bioessays* **7**: 173–175
- Hansen MD, Ehrlich JS, Nelson WJ (2002) Molecular mechanism for orientating membrane and actin dynamics to nascent cell-cell contacts in epithelial cells. *J Biol Chem* **277**: 45371–45376

Cytochalasin D and latrunculin B experiments

MIO cells were grown to 60% confluence on glass coverslips (Matek) and Cytochalasin D or Latrunculin B was added overnight at indicated concentrations. Cells were subsequently fixed and stained for the presence of annexin 2, Wave-1 or actin (using Cy5 phalloidin). Cells were examined at high power using a Leica AOBSP2 confocal microscope. In other experiments, cells were grown to 20% confluence and treated with siRNA with specificity for annexin 2, or with a control RNAi duplex that had been shown to have no effect on the level of expression of its target protein (annexin 5). Cells were cultured for 4 days after which time cytochalasin D or latrunculin B was added at various concentrations. Cells were then fixed and stained as before.

Labelling of actin barbed-ends with rhodamine actin

MTLn3 cells were grown overnight on acid-washed Matek dishes in DMEM with 5% FCS. Cells were starved in FCS-free media for 3 h and then treated with a final concentration of 5 nM EGF for 1–5 min. Nucleation sites (barbed ends) were localised using a previously described protocol (Chan *et al*, 1998) with slight modifications. In brief, the cells were permeabilised for 1 min in the presence of 0.45 μ M of rhodamine-labelled G-actin in buffer C (138 mM KCl, 10 mM Pipes, 0.1 mM ATP, 100 nM CaCl₂, 4 mM MgCl₂, pH 6.9) with 1% BSA and 0.025% saponin. After fixation and subsequent washes, rhodamine-actin incorporation was visualised directly by confocal microscopy.

Supplementary data

Supplementary data are available at *The EMBO Journal* Online.

Acknowledgements

We are especially grateful to Michael Way (CRUK Labs, London) for his critical evaluation of this work, Marie-France Carlier (Laboratoire d'Enzymologie et Biochimie Structurales, Gif Sur Yvette, France) for advice and guidance in protein purification, Astrid Limb for the MIO cells and Volker Gerke for the annexin 2 antibody. We also acknowledge the technical assistance of Keith Morris for the image analysis. This work was supported by grants from the Wellcome Trust, the Medical Research Council and Fight for Sight.

- Harder T, Gerke V (1993) The subcellular distribution of early endosomes is affected by the annexin IIp11(2) complex. *J Cell Biol* **123**: 1119–1132
- Harder T, Kellner R, Parton RG, Gruenberg J (1997) Specific release of membrane-bound annexin II and cortical cytoskeletal elements by sequestration of membrane cholesterol. *Mol Biol Cell* **8**: 533–545
- Hayes MJ, Merrifield CJ, Shao D, Ayala-Sanmartin J, D'Souza-Schorey C, Levine TP, Proust J, Curran J, Bailly M, Moss SE (2004a) Annexin 2 binding to phosphatidylinositol 4, 5 bisphosphate on endocytic vesicles is regulated by the stress response pathway. *J Biol Chem* **279**: 14157–14164
- Hayes MJ, Rescher U, Gerke V, Moss SE (2004b) Annexin–actin interactions. *Traffic* **5**: 571–576
- Higgs HN, Pollard TD (2001) Regulation of actin filament network formation through ARP2/3 complex: activation by a diverse array of proteins. *Annu Rev Biochem* **70**: 649–676
- Johnsson N, Marriott G, Weber K (1988) p36, the major cytoplasmic substrate of src tyrosine protein kinase, binds to its p11 regulatory subunit via a short amino-terminal amphiphatic helix. *EMBO J* **7**: 2435–2442
- Jones PG, Moore GJ, Waisman DM (1992) A nonapeptide to the putative F-actin binding site of annexin-II tetramer inhibits its calcium-dependent activation of actin filament bundling. *J Biol Chem* **267**: 13993–13997
- Jost M, Zeuschner D, Seemann J, Weber K, Gerke V (1997) Identification and characterization of a novel type of annexin-membrane interaction: Ca^{2+} is not required for the association of annexin II with early endosomes. *J Cell Sci* **110**: 221–228
- Knop M, Aareskjold E, Bode G, Gerke V (2004) Rab3D and annexin A2 play a role in regulated secretion of vWF, but not tPA, from endothelial cells. *EMBO J* **23**: 2982–2992
- Konig J, Gerke V (2000) Modes of annexin–membrane interactions analyzed by employing chimeric annexin proteins. *Biochim Biophys Acta* **1498**: 174–180
- Lee DB, Jamgotchian N, Allen SG, Kan FW, Hale IL (2004) Annexin A2 heterotetramer: role in tight junction assembly. *Am J Physiol Renal Physiol* **287**: 481–491
- Limb GA, Salt TE, Munro PM, Moss SE, Khaw PT (2002) *In vitro* characterization of a spontaneously immortalized human Muller cell line (MIO-M1). *Invest Ophthalmol Vis Sci* **43**: 864–869
- Mayran N, Parton RG, Gruenberg J (2003) Annexin II regulates multivesicular endosome biogenesis in the degradation pathway of animal cells. *EMBO J* **22**: 3242–3253
- Mejillano MR, Kojima S, Applewhite DA, Gertler FB, Svitkina TM, Borisy GG (2004) Lamellipodial versus filopodial mode of the actin nanomachinery: pivotal role of the filament barbed end. *Cell* **118**: 363–373
- Merrifield CJ, Rescher U, Almers W, Proust J, Gerke V, Sechi AS, Moss SE (2001) Annexin 2 has an essential role in actin-based macropinocytic rocketing. *Curr Biol* **11**: 1136–1141
- Nilius B, Gerke V, Prenen J, Szucs G, Heinke S, Weber K, Droogmans G (1996) Annexin II modulates volume-activated chloride currents in vascular endothelial cells. *J Biol Chem* **271**: 30631–30636
- Okuse K, Malik-Hall M, Baker MD, Poon WY, Kong H, Chao MV, Wood JN (2002) Annexin II light chain regulates sensory neuron-specific sodium channel expression. *Nature* **417**: 653–656
- Paavilainen VO, Bertling E, Falck S, Lappalainen P (2004) Regulation of cytoskeletal dynamics by actin-monomer-binding proteins. *Trends Cell Biol* **14**: 386–394
- Pollard TD, Borisy GG (2003) Cellular motility driven by assembly and disassembly of actin filaments. *Cell* **112**: 453–465
- Puisieux A, Ji J, Ozturk M (1996) Annexin II up-regulates cellular levels of p11 protein by a post-translational mechanisms. *Biochem J* **313**: 51–55
- Rescher U, Ruhe D, Ludwig C, Zobiack N, Gerke V (2004) Annexin 2 is a phosphatidylinositol (4,5)-bisphosphate binding protein recruited to actin assembly sites at cellular membranes. *J Cell Sci* **117**: 3473–3480
- Sakai E, Miyamoto M, Okamoto K, Kato Y, Yamamoto K, Sakai H (2001) Characterization of phagosomal subpopulations along endocytic routes in osteoclasts and macrophages. *J Biochem* **130**: 823–831
- Spudich JA, Watt S (1971) The regulation of rabbit skeletal muscle contraction. I. Biochemical studies of the interaction of the tropomyosin-troponin complex with actin and the proteolytic fragments of myosin. *J Biol Chem* **246**: 4866–4871
- van de Graaf SF, Hoenderop JG, Gkika D, Lamers D, Prenen J, Rescher U, Gerke V, Staub O, Nilius B, Bindels RJ (2003) Functional expression of the epithelial Ca^{2+} channels (TRPV5 and TRPV6) requires association of the S100A10–annexin 2 complex. *EMBO J* **22**: 1478–1487
- Zobiack N, Rescher U, Laarman S, Michgehl S, Schmidt MA, Gerke V (2002) Cell-surface attachment of pedestal-forming enteropathogenic *E. coli* induces a clustering of raft components and a recruitment of annexin 2. *J Cell Sci* **115**: 91–98